

Control of and Experimentation on an Active Dual-Mode Twisted String Actuation Mechanism

Seok Hwan Jeong, Kyung-Soo Kim, Member, *IEEE*, and Soohyun Kim

Abstract— In this paper, we present the control of and experimentation on an active dual-mode twisted string actuation mechanism for automatic transmission. This mechanism has a two-stage transmission ratio and is implemented by changing the twisted radius of the string in each mode (force mode or speed mode). Control algorithms for implementing different transmission ratios are proposed and experimentally verified. Moreover, this mechanism was able to change its compliance characteristics depending on the mode and it was also experimentally confirmed by impulse testing. Since this is a compact and simple transmission mechanism, it can be simply applied to small robotic system and provide a wide operating range and variable compliance.

I. INTRODUCTION

Over the past several decades, numerous advances have been made in the field of actuators. The energy efficiency of actuators has increased, and with the development of precision machining technology, small-sized actuators with high precision and their application have been developed in both academia and industry, such as shape memory alloys [1, 2], super-coiled polymers [3], pneumatic actuators [4], and hydraulic actuators [5]. Among these small actuators, electric motors are widely used for robotic applications [6, 7] because of their high stability and convenience. However, due to the high rotation speed and the low torque of the electric motors, a gearbox (a planetary or harmonic drive) capable of decelerating the rotational speed and amplifying the torque of the motor is required. These additional mechanical parts increase the volume, weight, and cost of the actuators and result in a low power transmission efficiency of approximately 60% for a planetary gear set with a high-reduction ratio. Single stage high reduction ratio gears such as in harmonic and cycloid drives have a power transmission efficiency of approximately 70 to 80% [8], which is higher than planetary gears, but they are difficult to miniaturize due to the complexity of their mechanical parts

To overcome these shortcomings and replace the gearbox transmission mechanism, a twisted string actuation (TSA) mechanism has been proposed and studied [9-12]. The TSA mechanism is rotary-to-linear transmission that produces a

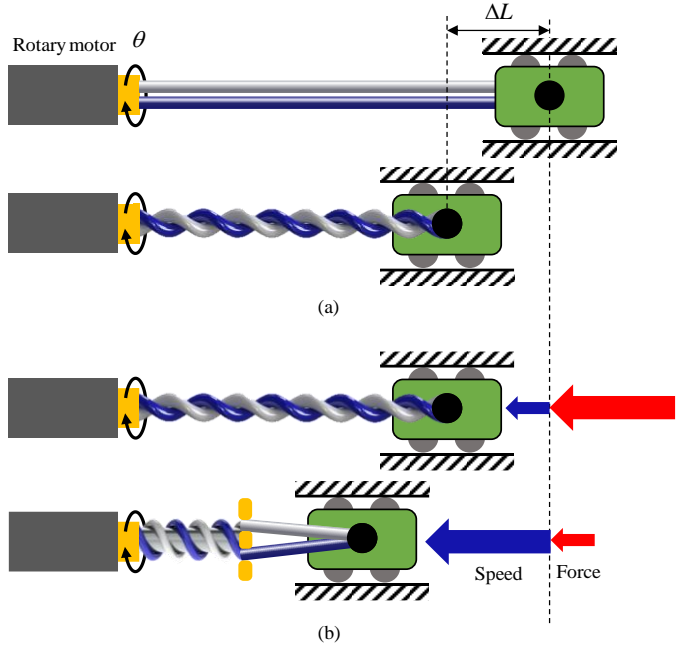


Figure 1. (a) Concept of the twisted string actuation (TSA) and (b) variable transmission ratio depending on the twisted radius.

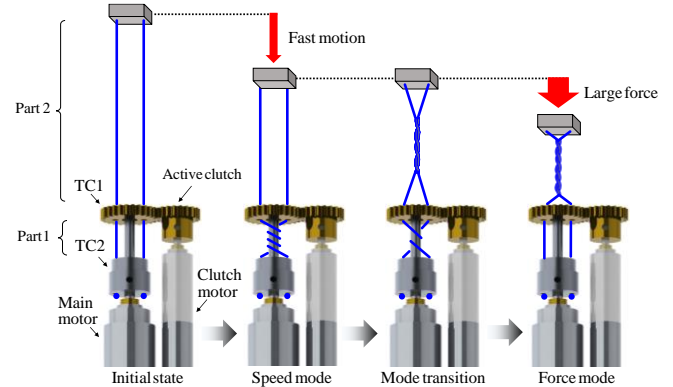


Figure 2. Drive mechanism of the active dual-mode TSA [17].

remarkably high transmission ratio by twisting a single string or a pair of strings with a high power transmission efficiency of approximately 90% [12], as shown in Fig. 1 (a). Therefore, it can substantially reduce the speed of the motor and amplify the contraction force with very lightweight and compact mechanical components without a bulky gearbox. Since the strings play the roles of both driveline and transmission, the weight and volume of the whole system can be considerably reduced, and it is suitable for a mechanism having a very narrow space, such as a robotic finger. Since the rotary motion is directly converted into linear motion in a direction parallel

This study was supported by the Technology Innovation Program (10051330), which was funded by the Ministry of Trade, Industry & Energy (MI, Korea) and the National Research Foundation of Korea(NRF) grant funded by the Korea government(MEST) (No. NRF-2017R1A2B3010253)

Seok-Hwan Jeong, Kyung-Soo Kim, and Soohyun Kim are with the Mechanical Engineering Department, Korea Advanced Institute of Science and Technology (KAIST), Daejeon, 305-701, Republic of Korea (e-mail:astroidbelt@kaist.ac.kr; kyungsookim@kaist.ac.kr; soohyun@kaist.ac.kr)

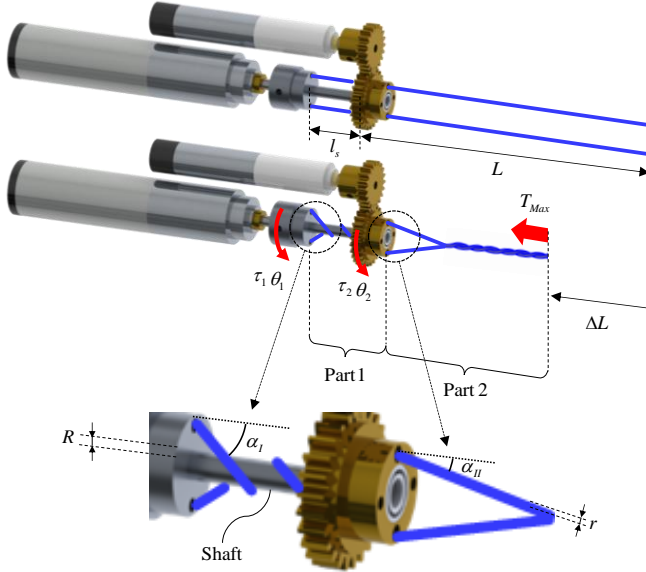


Figure 3. Driving mechanism of the active dual-mode TSA mechanism.

to the motor shaft, the mechanical design can be simplified for tendon-based robots.

While the TSA mechanism has a number of advantages, it suffers from slow contraction speed and has a fixed transmission ratio, thus it does not have a wide operating range (e.g. large force or fast speed). To resolve this issue, we previously proposed a passive dual-mode TSA mechanism [13, 14] and an active dual-mode TSA mechanism [15-17] that can control the transmission ratio by changing the twisted radius of the string, as shown in Fig. 2. The proposed active dual-mode TSA mechanism can generate fast contraction motion (speed mode) or a large contraction force (force mode) depending on which parts of the strings are twisted (Part 1 or Part 2 in Fig. 2). The twisting parts are determined by relative rotary motion of the twisted coupler (TC)1 and TC2, which are controlled by the main motor and the clutch motor. This mechanism significantly increases the speed-force range and mitigates the slow contraction speed, which was a problem with the existing TSA. However, the active dual-mode TSA mechanism uses two motors for one output, so various control algorithms are needed depending on the twisting mode.

In this paper, we present general control algorithms and experiments for the active dual-mode TSA mechanism in force mode, speed mode, and mode transition. This paper is organized as follows. In Section II, the active dual-mode TSA mechanism is introduced. Section III is devoted to the control algorithms for various twisting modes and experiments with it are also presented. Experiments on the compliance characteristics of each twisting mode are covered in Section IV, and a discussion of the results and conclusions about the study are provided in Sections V and VI, respectively.

II. ACTIVE DUAL-MODE MECHANISM

A. The Driving Mechanism

Fig. 3 shows the driving mechanism of the active dual-mode TSA mechanism. The final contraction force T_{max}

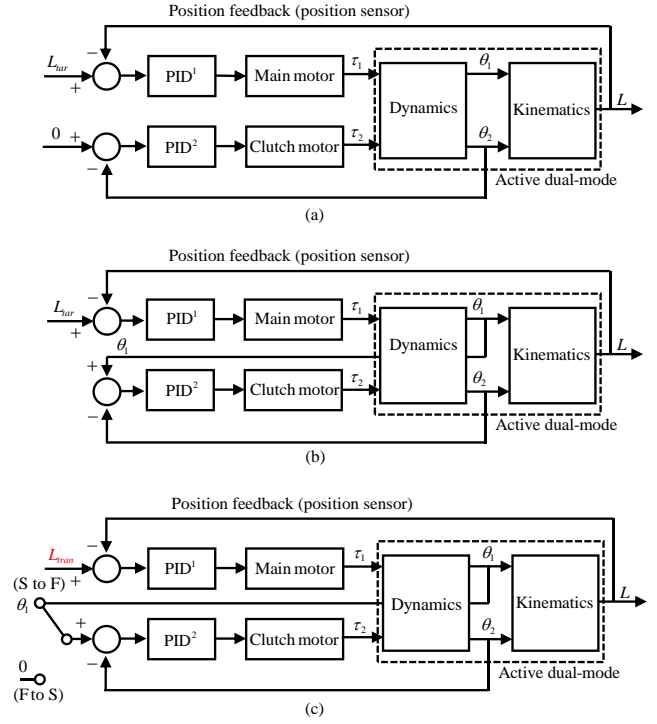


Figure 4. Control algorithms of the active dual-mode TSA mechanism for (a) speed mode, (b) force mode and (c) mode transition. ‘S to F’ means ‘speed mode to force mode’ and ‘F to S’ means ‘force mode to speed mode’.

according to the rotation angle of TC1 θ_1 and the rotation angle of TC2 θ_2 is derived as follows [17]:

$$T_{max}(\alpha_I, \alpha_{II}) = \min \left[\frac{\cos \alpha_{II}}{R \cdot \sin \alpha_I} \tau_1, \left[\frac{\tau_2}{r \tan \alpha_{II} - R \frac{\sin \alpha_I}{\cos \alpha_{II}}} \right] \right], \quad (1)$$

where R and r_s are the radii of the shaft and the string, respectively, τ_1 and τ_2 are the torques of the main motor and clutch motor, respectively, and, α_I and α_{II} are the angles of inclination of the string in Part 1 and Part 2, respectively, as shown in Fig. 3.

According to (1), T_{max} can be changed by adjusting α_I and α_{II} , which means that it works like a transmission that can change the speed-force ratio. Assuming that the radius of the string r is much smaller than the radius of the shaft R ($r \ll R$), then α_I should be close to zero ($\alpha_I \approx 0$) to increase the transmission ratio (force mode, maximize T_{max}) and α_{II} should be close to zero ($\alpha_{II} \approx 0$) to decrease the transmission ratio (speed mode, minimize T_{max}). Structurally, $\alpha_I \approx 0$ equals $\theta_1 \approx \theta_2$, and $\alpha_{II} \approx 0$ equals $\theta_2 \approx 0$, so the transmission ratio is adjustable by controlling the rotation angle of the main motor θ_1 and the clutch motor θ_2 .

III. THE CONTROL ALGORITHMS

For practical use, the active dual-mode TSA mechanism should implement driving modes having different transmission ratios such as speed mode, force mode, and the transition between the two. Therefore, several control loops are required for each case, as shown in Fig. 4. In speed mode,

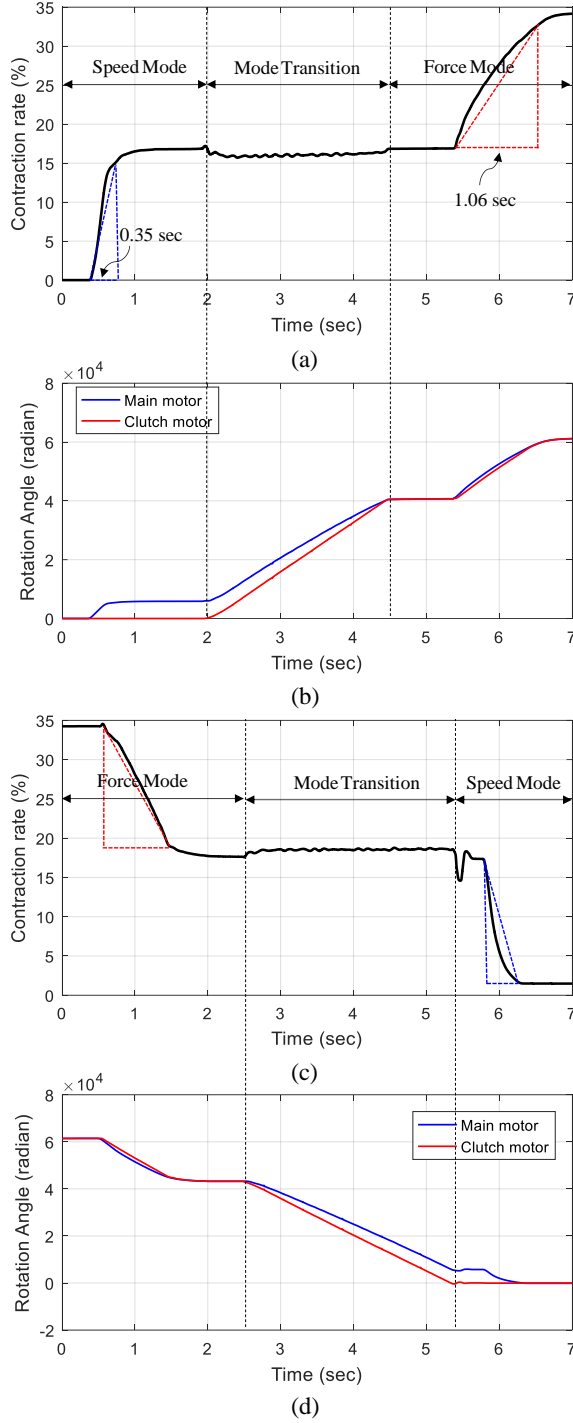


Figure. 5. Experimental results for the control algorithm: (a) and (b) – contraction motion, and (c) and (d) – extension motion.

the final output position of the active dual-mode TSA mechanism L is fed back to the main motor to reach the desired target position L_{tar} , as shown in Fig. 4 (a). At that time, the clutch motor is controlled so that θ_2 is always kept at 0. In force mode, L is also fed back to the main motor to reach L_{tar} , and θ_1 is set to the reference of the clutch motor so that θ_1 and θ_2 are equal, as shown in Fig. 4 (b). In these control algorithms, the main motor serves to control the position of the system L and the clutch motor serves to control the twisting

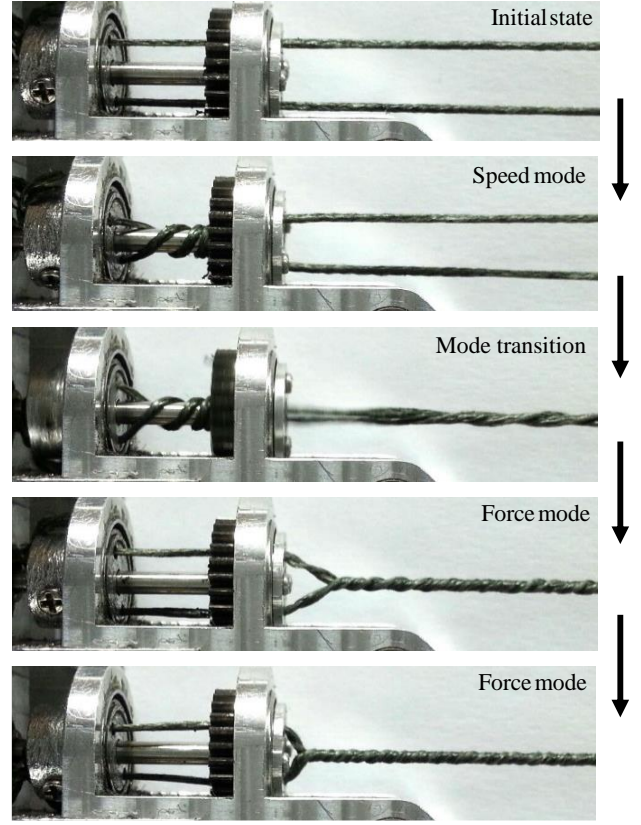


Figure. 6. Experimental results on the control algorithms for twisting during mode transition

TABLE I
SPECIFICATIONS OF THE EXPERIMENT PARAMETERS

Items	Specification
Size	69.2 mm x 19.5 x 15 mm
Weight	42.6 g
Motor 1	Maxon motor (315170)
	Continuous torque, M_{m1} : 1.74 mNm
	k_1 : 64:1 gear, ϕ 10, 8 W
Motor 2	Maxon motor (455020)
	Continuous torque, M_{m2} : 0.354 mNm
	k_2 : 57:1(motor) x 13:10(TC2) gear, ϕ 6, 1.5 W
String radius, r	0.2 mm
Shaft radius, R	1 mm
Length of shaft, l_s	7.7 mm
Total length of string, L	89 mm
String material	Spectra

for the particular mode by determining where the twisting occurs in Part 1 or Part 2. In mode transition, position L_{tran} is fed back to the main motor to maintain a constant position, as shown in Fig. 4 (c). Subsequently, the clutch motor has a different reference depending on the direction of the mode transition (speed mode to force mode (S to F) or force mode to speed mode (F to S)).

Fig. 5 shows experimental results of twisting on each mode and mode transition using the control algorithms. Specifications of the experimental parameters are summarized in Table I. Fig. 5 (a) and (b) shows the contraction rate and rotation angle of the main motor and the clutch motor,

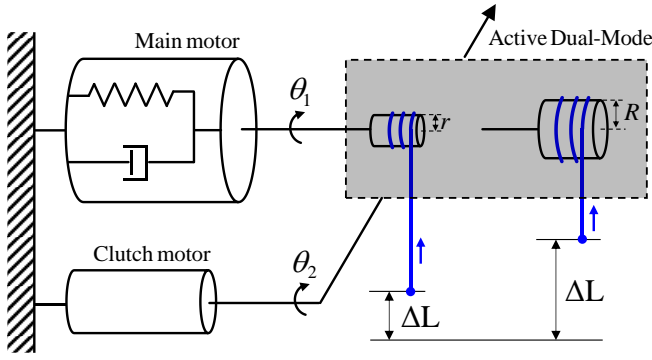


Figure. 7. The transmission ratio (the twisted radius of the string) of the active dual-mode TSA mechanism changed by control of the clutch motor. At low transmission ratio, the compliance of the main motor can be used to increase the compliance of the system.

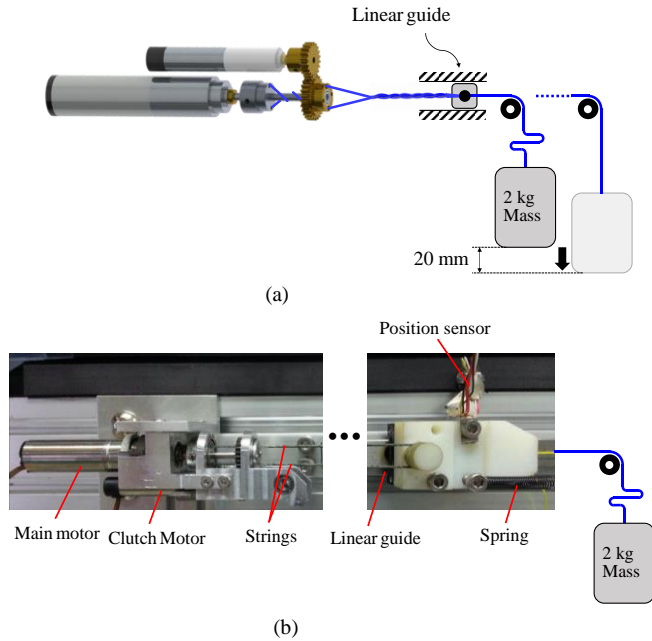


Figure. 8. (a) Experimental concept and (b) setup

respectively, in contraction motion. On the other hand, Fig. 5 (c) and (d) shows the case of extension motion. During speed mode, the clutch motor was stopped and only the main motor rotated, as shown in Fig. 5 (b), resulting in twisting in Part 1 and rapid contraction; it took approximately 0.35 sec to reach 15% contraction of the total string length, as shown in Fig. 5 (a). On the other hand, in force mode, the rotation of the main motor and the clutch motor were synchronized to produce twisting in Part 2, resulting in slow contraction; it took approximately 1.05 sec to reach 15% contraction. Experimental results show that the proposed control loop successfully operated twisting for each mode and had approximately 3 times the transmission ratio shifting effect between speed mode and force mode.

In the mode transition process, the control loop of Fig. 4 (c) is used to switch the twisting between modes while maintaining the current position. As shown in Fig. 5 (b), the

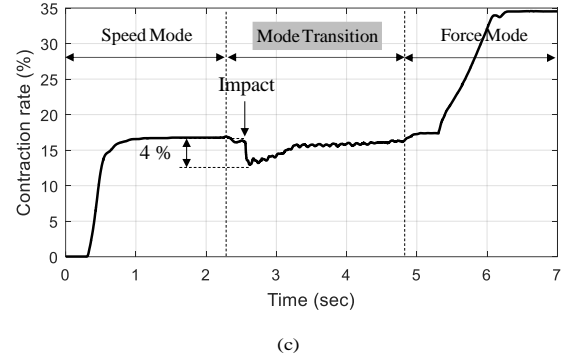
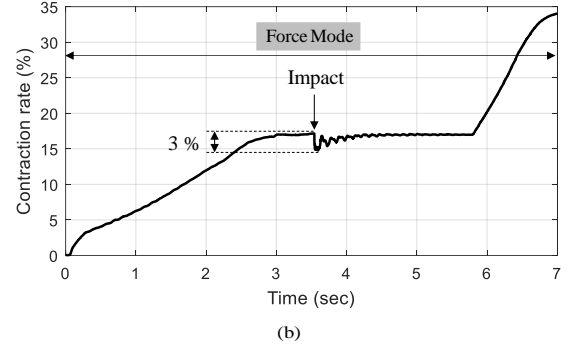
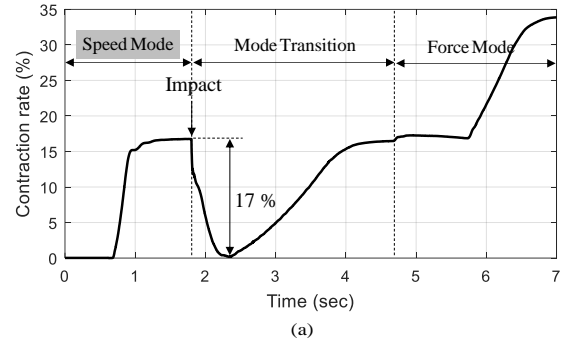


Figure. 9. Experimental results for the compliance test for (a) speed mode, (b) force mode, and (c) mode transition.

rotation of the clutch motor and the main motor were controlled to be at the same rotation angle, and at the same time, the twisting in Part 1 was transferred to Part 2 to maintain the current position, as shown in Fig. 6.

IV. COMPLIANCE

In this chapter, we experimentally verify the transmission ratio shifting effect of the proposed mechanism by investigating the compliance characteristics of twisting for each mode.

Systems such as robotic hands, which have a lot of interaction with external environments, are frequently subjected to unpredictable impacts. This impulse-type impact cannot be compensated for in a controlled manner because the impact greatly exceeds the control bandwidth of the actuator and can cause serious damage to the drive parts. Therefore, it is important to have a passive element such as compliance and back-drivability characteristics to absorb the impact and protect the system.

In [18], additional mechanical parts such as springs, cam disks, and rollers and the actuator were added to implement a variable stiffness (compliance) mechanism in a robotic hand that was able to continuously change and had excellent shock absorbing performance. However, this mechanism may have increased the overall size of the system due to the large number of mechanical parts. On the other hand, the active-dual mode TSA mechanism simplifies and miniaturizes the compliance mechanism by changing the transmission ratio and using the compliance of the actuator itself. The compliance and back-drivability characteristics of the system can be changed by adjusting the transmission ratio of the active dual-mode TSA mechanism, as shown in Fig. 7. At a high transmission ratio (force mode), the output force is amplified and the system has low compliance, while it has high compliance at a low transmission ratio (speed mode). Therefore, we expect that the variable compliance could be implemented by changing twisting mode during mode transition.

In the experiment, a sudden impact was applied to the active dual-mode TSA module for each mode (speed mode, force mode, and mode transition), as shown in Fig. 8. A mass of 2 kg was connected to the actuator with a string, which was dropped to 20 mm and impacted the active dual-mode TSA module.

Fig. 9 shows the experimental results. In speed mode, the actuator was not able to maintain its original position and was driven in reverse, releasing 17% of string length, as shown in Fig. 8 (a). However, Fig. 9 (b) and (c) shows that, while maintaining the original position, only 3% and 4% of reverse driving were generated in force mode and mode transition, respectively, in comparison with speed mode.

V. DISCUSSION

The experimental results in section IV show the back-drivability characteristics of the active dual-mode TSA mechanism for twisting in the various modes. Back-drivability is related to the compliance of the actuator, and in this experiment, high back-drivability can be said to mean high compliance. Considering the effect of tension on string extension, speed mode produces considerably greater compliance than force mode.

In these experiments, the force applied to the actuator was not directly measured but could be estimated from the time to reach the saturation point under the same impulse conditions. From the experimental results, we can infer that force mode absorbs the impulse for a shorter time, causing a larger impulsive force, while speed mode absorbs the impulse for a relatively longer time, resulting in a smaller impulsive force.

The compliance characteristics of the active dual-mode TSA mechanism could be used in robotic hands since, in speed mode, a robot hand could perform high-speed operations with a low transmission ratio and effectively absorb a large impulse. In force mode, it is possible to generate a large grasping force with high a transmission ratio and suitable for

precision work requiring high stiffness (low compliance). Switching between these operating modes can be easily carried out by the mode transition control algorithms depending on the situation.

Despite these advantages, there are problems to be solved. As shown in Fig. 5 (a), it took more than 2 sec for twisting to switch between modes, thus instantaneous transmission ratio switching is impossible and it is difficult to cope with sudden changes. In addition, the mechanism has a short stroke in force mode. To overcome these problems, an additional clutch mechanism (like a dog clutch) is required to change the transmission ratio instantaneously and separate the twisting for each mode. In addition, as with all TSA mechanisms, the issue of low durability must be addressed.

VI. CONCLUSIONS

In this paper, we introduce an active dual-mode TSA mechanism, which is a transmission mechanism based on twisted string actuation, and several control algorithms to implement the two-stage transmission ratio are proposed. In addition, experiments were conducted to verify the mechanism's compliance under different transmission ratios of twisting for each operating mode (speed, force, and transition).

Future studies will focus on modifying the clutch mechanism for instant transmission ratio shifting and increasing string durability.

REFERENCES

- [1] K. Ikuta, "Micro/miniature shape memory alloy actuator," in *Robotics and Automation, 1990. Proceedings., 1990 IEEE International Conference on*, 1990, pp. 2156-2161.
- [2] K. Andrianesis and A. Tzes, "Development and Control of a Multifunctional Prosthetic Hand with Shape Memory Alloy Actuators," *Journal of Intelligent & Robotic Systems*, vol. 78, pp. 257-289, May 2015.
- [3] M. C. Yip and G. Niemeyer, "High-performance robotic muscles from conductive nylon sewing thread," in *Robotics and Automation (ICRA), 2015 IEEE International Conference on*, 2015, pp. 2313-2318.
- [4] R. Deimel and O. Brock, "A compliant hand based on a novel pneumatic actuator," in *Robotics and Automation (ICRA), 2013 IEEE International Conference on*, 2013, pp. 2047-2053.
- [5] S. Guitao, S. Junpeng, D. Xiang, and W. Xiaojing, "Hydraulic robot force control based on environment parameters adaptive estimation," *Journal of Huazhong University of Science and Technology (Natural Science Edition)*, vol. 4, p. 006, 2015.
- [6] H. Liu, P. Meusel, N. Seitz, B. Willberg, G. Hirzinger, M. H. Jin, *et al.*, "The modular multisensory DLR-HIT-Hand," *Mechanism and Machine Theory*, vol. 42, pp. 612-625, May 2007.
- [7] M. S. Johannes, J. D. Bigelow, J. M. Burck, S. D. Harshbarger, M. V. Kozlowski, and T. Van Doren, "An overview of the developmental process for the modular prosthetic limb," *Johns Hopkins APL Technical Digest*, vol. 30, pp. 207-216, 2011.
- [8] J. W. Sensinger and J. H. Lipsey, "Cycloid vs. harmonic drives for use in high ratio, single stage robotic transmissions," in *Robotics and Automation (ICRA), 2012 IEEE International Conference on*, 2012, pp. 4130-4135.
- [9] M. Shoham, "Twisting wire actuator," *Journal of Mechanical Design*, vol. 127, pp. 441-445, May 2005.
- [10] T. Würtz, C. May, B. Holz, C. Natale, G. Palli, and C. Melchiorri, "The twisted string actuation system: Modeling and control," in *Advanced Intelligent Mechatronics (AIM), 2010 IEEE/ASME International Conference on*, 2010, pp. 1215-1220.

- [11] T. Sonoda and I. Godler, "Position and force control of a robotic finger with twisted strings actuation," in *Advanced Intelligent Mechatronics (AIM), 2011 IEEE/ASME International Conference on*, 2011, pp. 611-616.
- [12] I. Gaponov, D. Popov, and J. H. Ryu, "Twisted String Actuation Systems: A Study of the Mathematical Model and a Comparison of Twisted Strings," *Ieee-Asme Transactions on Mechatronics*, vol. 19, pp. 1331-1342, Aug 2014.
- [13] Y. J. Shin, H. J. Lee, K. S. Kim, and S. Kim, "A Robot Finger Design Using a Dual-Mode Twisting Mechanism to Achieve High-Speed Motion and Large Grasping Force," *Ieee Transactions on Robotics*, vol. 28, pp. 1398-1405, Dec 2012.
- [14] H. J. Lee, J.-K. Ryu, J. Kim, Y. J. Shin, K.-S. Kim, and S. Kim, "Design of modular gripper for explosive ordinance disposal robot manipulator based on modified dual-mode twisting actuation," *International Journal of Control, Automation and Systems*, vol. 14, pp. 1322-1330, 2016.
- [15] S. H. Jeong, Y. J. Shin, K.-S. Kim, and S. Kim, "Dual-Mode Twisting Actuation Mechanism with an Active Clutch for Active Mode-Change and Simple Relaxation Process," in *IEEE/RSJ International Conference on Intelligent Robots and Systems*, 2015.
- [16] S. H. Jeong, K.-S. Kim, and S. Kim, "Development of a robotic finger with an active dual-mode twisting actuation and a miniature tendon tension sensor," in *Advanced Intelligent Mechatronics (AIM), 2016 IEEE International Conference on*, 2016, pp. 1-6.
- [17] S. H. Jeong, K.-S. Kim, and S. Kim, "Designing Anthropomorphic Robot Hand with Active Dual-Mode Twisted String Actuation Mechanism and Tiny Tension Sensors," *IEEE Robotics and Automation Letters*, vol. PP, pp. 1-1, 2017.
- [18] M. Grebenstein, A. Albu-Schäffer, T. Bahl, M. Chalon, O. Eiberger, W. Friedl, *et al.*, "The DLR hand arm system," in *Robotics and Automation (ICRA), 2011 IEEE International Conference on*, 2011, pp. 3175-3182.